Smectic-A-filled birefringent elements and fast switching twisted dual-frequency nematic cells used for digital light deflection

Oleg Pishnyak, MEMBER SPIE
Kent State University
Chemical Physics Interdisciplinary Program
P.O. Box 5190
Kent, Ohio 44242-0001

Andrii Golovin, MEMBER SPIE
Kent State University
Liquid Crystal Institute
P.O. Box 5190
Kent, Ohio 44242-0001

Liubov Kreminska
Truman State University
Kirksville, Missouri 63501

John J. Pouch
Félix A. Miranda
NASA John H. Glenn Research Center
21000 Brookpark Road
Cleveland, Ohio 44135

Bruce K. Winker
Rockwell Scientific Company LLC
1049 Camino Dos Rios
Thousand Oaks, California 91360

Oleg D. Lavrentovich, FELLOW SPIE
Kent State University
Liquid Crystal Institute
Chemical Physics Interdisciplinary Program
P.O. Box 5190
Kent, Ohio 44242-0001
E-mail: odl@lci.kent.edu

Abstract. We describe the application of smectic A (SmA) liquid crystals for beam deflection. SmA materials can be used in digital beam deflectors (DBDs) as fillers for passive birefringent prisms. SmA prisms have high birefringence and can be constructed in a variety of shapes, including single prisms and prismatic blazed gratings of different angles and profiles. We address the challenges of uniform alignment of SmA, such as elimination of focal conic domains. Fast rotation of the incident light polarization in DBDs is achieved by an electrically switched 90-deg twisted nematic (TN) cell. © *2006 Society of Photo-Optical Instrumentation Engineers.* [DOI: 10.1117/1.2192520]

Subject terms: beam deflector; smectic A; polarization rotator; birefringent prism.

Paper 050419R received May 25, 2005; revised manuscript received Sep. 1, 2005; accepted for publication Sep. 8, 2005; published online Apr. 28, 2006.

1 Introduction

Beam steering devices are in a great demand in free-space laser communications, optical fiber communications, optical switches, scanners,[1–5] etc. In addition to mechanical devices such as gimbals and mirrors, a number of other techniques are under development, such as ceramic-based phase gratings,[2] microelectromechanical relief gratings,[3] micromirror devices,[4] decentered lens arrays, thermo-optic deflectors,[5] photonic crystals,[6] etc. Liquid crystals (LCs) are of special interest as active materials in nonmechanical beam steerers and deflectors, because they promise low size, weight, operating voltage, and low-cost fabrication.[1,7] Recent advances in the synthesis of new LC materials[8] and in the design of nematic LC cells[9] significantly improved parameters important for effective beam steering, such as optical birefringence and response time.

One of the most promising areas for LC-based systems is NASA's near-Earth and deep-space missions that require precise, diffraction-limited (submicroradian), electronic (nonmechanical) beam steering as well as *in situ* wavefront correction. LC-based systems are inexpensive, lightweight, and use low power. LC optical phased arrays could be used as part of a tracking network that supports high-data-rate communication links between the planetary rovers, the host lander, the orbiting spacecraft, and space platforms; autonomous operation of the rovers and robotic systems; and possibly strategic mining operations.

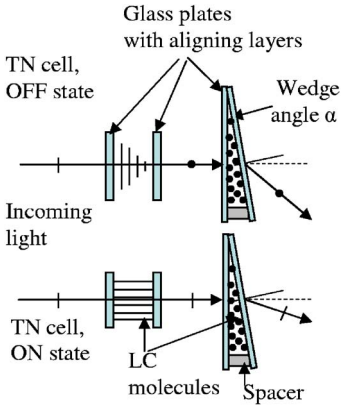

Fig. 1 Principal scheme of a beam deflecting stage, composed of the switchable polarization rotator (90-deg TN cell) and a passive prism made of a SmA wedge. Both elements can be replaced. For example, a crystalline prism can be used as a deflector, or an electrically controlled birefringence cell can be used as a polarization rotator.

The most popular liquid crystal-based beam steering devices are based on diffractive and prismatic designs. Diffractive LC devices have been known since at least 1974, when Borel et al. described a binary rectangular LC diffraction grating.[10] This approach has been expanded by optical array beam steerers,[1,11–14] polymer-dispersed liquid crystal gratings,[15] ferroelectric liquid crystal gratings,[16] photonic crystals filled with liquid crystals,[6] and voltage-controlled cholesteric liquid crystal gratings capable of both Raman-Nath and Bragg diffraction.[17,18]

Among the prism-based digital beam deflectors (DBDs), one of the most effective designs uses a cascade of elementary stages, each of which represents a pair consisting of an active polarization rotator and a prismatic deflector.[19–26] The advantage of such a decoupled design is that it allows one to separate the issue of the short response time (determined mostly by the switching speed of the rotator) and the angular range of deflection (determined by the geometry and optical properties of the deflector). For example, the active element can be electrically switched by a 90-deg twisted nematic (TN) cell, followed by a passive birefringent prism that separates the beam into two channels, depending on the beam polarization (Fig. 1). Depending on the applied voltage, the TN cell rotates the polarization of incident light by $\pi/2$ (no field, OFF state) or leaves the polarization intact (when the applied electric field reorients the liquid crystal molecules perpendicular to the plates of the cell, ON state). Inside the prism, the beam propagates in ordinary or extraordinary mode, depending on the polarization. As the ordinary and extraordinary refractive indices are different, the two modes of propagation through the prism result in different angles of deflection. As is clear from Fig. 1, if the Smetic A (SmA) prism is used, the optical axis (and thus the preferred orientation of the SmA molecules) should be aligned along the edge of the wedge. In this geometry, the director field is uniform everywhere. The decoupled pair of rotator and deflector has no moving parts and can be cascaded into N stages, making 2^N addressable beam directions.[19–26]

The liquid crystals can be used in both active and passive elements of prism-based DBDs, as they demonstrate a relatively high optical birefringence (in the range 0.1 to 0.4) and relatively fast switching speeds (milliseconds or less) (see, for example, Ref. 9). Application of LCs for polarization switching is a well-developed field, mostly because the TN and similar nematic cells are at the heart of modern LC display devices.[27]

Application of LCs in the passive prismatic elements is less studied despite their apparent advantages, such as structural flexibility and low-cost fabrication. One of the reasons for such a neglect is that a LC-based prism with a substantial dihedral angle α (needed for the substantial angle of beam deflection) and a substantial aperture A should be relatively thick, up to $h=A\tan\alpha$. If h is in the range of millimeters and centimeters, then huge losses caused by light scattering at director fluctuations[28,29] rule out the applicability of the nematic LCs. In this work, we describe passive prismatic elements formed by a uniaxial SmA LC. The advantage of the SmA materials over nematic LCs is that director fluctuations are suppressed by the layered smectic structure.

The work is organized as follows. Section 2 discusses the alignment procedures of SmA. Section 3 presents the optical properties of single prisms and arrays of polymer prisms filled with SmA. Section 4 describes the electro-optical properties of 90-deg TN cells filled with dual-frequency nematic. Discussion and conclusions are presented in Secs. 5 and 6, respectively.

2 Smetic-A Liquid Crystal Materials

In SmA, the elongated rod-like molecules are arranged in a periodic stack of layers with the director **n** (a unit vector that shows the average local direction of molecules and thus the optic axis of the material) being perpendicular to the layers; the states **n** and **−n** are identical. Inside the layer, the molecular centers of gravity show no long-range order, thus each layer is a 2-D fluid. Positional order along **n** significantly reduces thermal director fluctuations and thus reduces light scattering.[28,29] However, the very same layered structure brings about another possible source of scattering, namely, static director distortions such as undulations and focal conic domains (FCDs).[30–33] The problem is especially pronounced for the highly birefringent cyanobiphenyl materials, in which the molecules form partially overlapped pairs with oppositely oriented dipole moments. The thickness of smectic layers in these materials is about 1.4 to 1.6 of the length of an individual molecule and can vary significantly with temperature; the changes in layer thickness result in director distortions. For example, cooling of the SmA material 4-octyloxy-4′-cyanobiphenyl (8OCB) in the planar cell with polyisoprene-coated substrates[34] results in layer undulations and formation of FCDs clearly visible in Fig. 2. These FCDs can be stabilized by a mechanical impurity in the bulk or at the surface of the cell.[30] In principle, one can use a magnetic field to align the SmA sample uniformly.[31,32] We quantify the process of field alignment of SmA by considering the behavior of an isolated FCD. The method might be effective if large magnetic fields are available. The model predicts that for each value of the applied field, there is a characteristic size of the FCD below which the domain cannot be transformed into the uniform state.

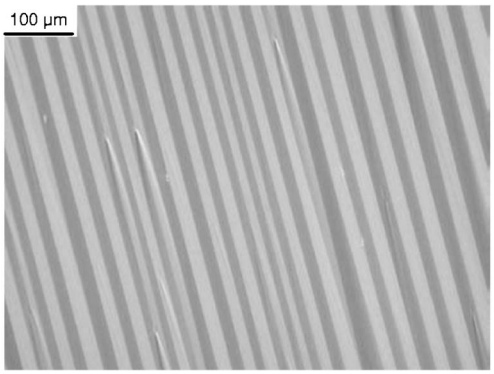

Fig. 2 Polarizing-microscope texture of an undulation pattern in SmA material 8OCB created by periodic director variations. The SmA was cooled down from the magnetically aligned nematic phase. Aligning layer: polyisoprene, no rubbing.[34] Cell thickness of 5 μm.

To obtain a close estimate of the magnetic field needed to align the SmA uniformly, we consider the simplest type of FCD, the so-called toric FCD, that can be stabilized by a foreign particle in the SmA bulk.[35,36] The toric FCD is based on a pair of linear defects, a circular defect line, and the straight line passing through the center. The smectic layers are wrapped around the pair, as shown in Fig. 3. Note that outside the FCD, the molecules are oriented uniformly along a single axis parallel to the plates.

Suppose a small toric FCD with the radius a of the defect circle, much smaller than the lateral size of the cell, is stabilized in an otherwise uniform SmA sample by a particle, which sets tangential orientation of SmA molecules at its surface. For the sake of simplicity, we approximate the particle by a disk of radius R (Fig. 3). If the SmA were uniform, the director would be in an unfavorable perpendicular orientation at the plate. The FCD would be stable if its elastic energy,[37]

$$F_{el} = 2\pi^2 aK[\ln(2a/r_c) - 2 - \bar{K}/K] + F_c, \tag{1}$$

(where K is the splay elastic constant, $\bar{K}$ is the saddle-splay constant, r_c is the core radius of the circular defect, and F_c is the core energy of the circle and the straight line) is smaller than the anchoring energy difference between the FCD-free (uniform) state and the FCD state:

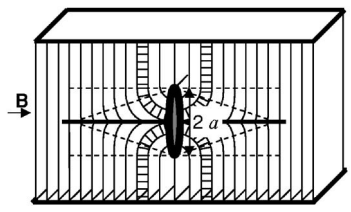

Fig. 3 Schematic view of toric FCD. The SmA layers are perpendicular to the substrates and folding within the FCD. The director changes the orientation on 90 deg from tangential outside the FCD to vertical within the FCD to satisfy the boundary conditions at the disk-like foreign particle in the SmA bulk.

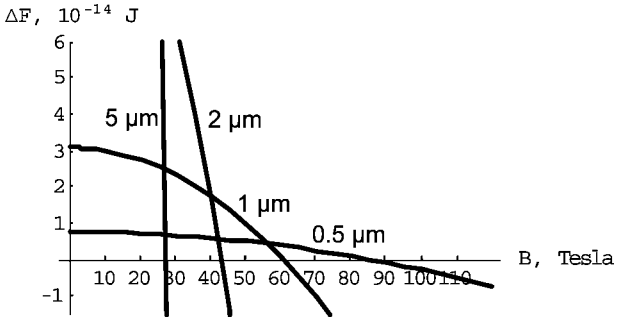

Fig. 4 Free energy difference between the uniform state of a SmA slab with an incorporated foreign particle disk and the state with the toric FCD as a function of the magnetic field applied to align the director uniformly. Different curves corresponding to the size of FCDs equal 0.5, 1, 2, and 5 μm.

$$\Delta F_s = 2\pi a^2 W, \tag{2}$$

where W is the (polar) surface anchoring coefficient at the SmA-particle interface. In SmA, $W \sim (10^{-3} - 10^{-2})$ J/m^2 is higher than the corresponding value in the nematic phase, $W \sim (10^{-5} - 10^{-4})$ J/m^2.[38]

If the anisotropy $\chi_a = \chi_\parallel - \chi_\perp > 0$ of SmA diamagnetic susceptibility is positive, then applying the field in the direction of the desired orientation of molecules should reduce the FCD, as the molecules inside the domain should reorient along **B** (Fig. 3). The diamagnetic energy gain from such a reorientation is

$$\Delta F_B = 2\int \frac{1}{2}\mu_0^{-1}\chi_a B^2 \sin^2\theta dV,$$

where $\mu_0 = 4\pi \cdot 10^{-7}$ N/A^2 is the permeability of free space, θ is the angle between the director and **B**, the volume element is $dV = r(a - r\sin\theta)\sin\theta d\theta d\varphi dr$; r and $r - a/\sin\theta$ are the principal radii of curvature of SmA layers within the toric FCD, and r varies in the range from 0 to $a/\sin\theta$; $0 \leqslant \theta \leqslant \pi/2$; and $0 \leqslant \varphi < 2\pi$. Integration yields

$$\Delta F_B = \frac{1}{3}\pi\mu_0^{-1}\chi_a B^2 a^3. \tag{3}$$

The stability of the FCD is determined by the energy difference between the uniform state and the FCD state, comprised of the elastic, surface anchoring, and diamagnetic contributions, $\Delta F = \Delta F_s - F_{el} - \Delta F_B$:

$$\Delta F = 2\pi a^2 W - 2\pi^2 aK\left(\ln\frac{2a}{r_c} - 2 - \frac{\bar{K}}{K}\right) - F_c - \frac{1}{3}\pi\mu_0^{-1}\chi_a B^2 a^3. \tag{4}$$

Figure 4 shows the function $\Delta F(B)$ for four different sizes of FCDs, of radius $a = 0.5$, 1, 2, and 5 μm, calculated for the following typical values of parameters[29,38]: $K = 10^{-11}N$, $\bar{K} = 0$, $W = 5^{*}10^{-3}$ J/m^2, $r_c = 10$ nm, $F_c = 0$ (r_c is chosen to adsorb the core energy into the elastic energy of layer distortions[28]), and $\chi_a = 10^{-5}$. The plot demonstrates that for each value of a, there is a critical value of the field

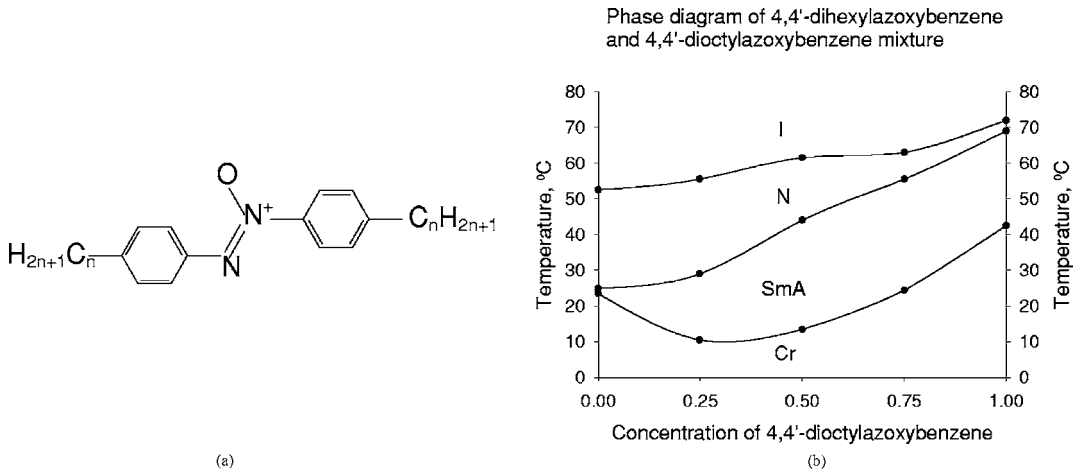

Fig. 5 (a) Molecular structure of 4,4′-*n*-dialkylazoxybenzene. (b) Phase diagram of the binary mixture of $n=6$ and $n=8$ homologues of 4,4′-*n*-dialkylazoxybenzene.

for which ΔF becomes negative, i.e., the uniform state is energetically preferred over the FCD state. The higher the field, the smaller the size of the FCDs that can be transformed into the uniform state. However, to reduce the size of FCD to a practical subwavelength value, say, $a=0.5-1$ μm, one needs huge magnetic fields of the order of tens and hundreds of Tesla (Fig. 4). The alignment can be assisted by applying the magnetic field while the material is in the nematic phase, and then cooling it down to the SmA phase, as the surface anchoring in the nematic phase is much weaker than in the SmA phase.

The magnetic field needed to realign the director around the foreign inclusion in the nematic phase can de determined from the condition that the diamagnetic coherence length,

$$\xi = \frac{1}{B}\sqrt{\frac{\mu_0 K}{\chi_a}},$$

is smaller than the anchoring extrapolation length $l=K/W$:

$$B_c = W\sqrt{\frac{\mu_0}{K\chi_a}}. \tag{5}$$

For example, $B\sim 1$ T would be sufficient to suppress the director distortions around a particle with $W\sim 10^{-5}$ J/m^2; $B\sim 10$ T would be needed if $W\sim 10^{-4}$ J/m^2; etc. Therefore, magnetic alignment is easier in the nematic phase than in the SmA phase.

Consideration suggests that to minimize light losses, one should search for the SmA material composed of nonpolar molecules in which the molecules do not form pairs, and the layer thickness does not change much with temperature and in which there is a nematic phase, in addition to the SmA phase. The requirements are met by low-molecular weight materials belonging to the class of 4,4′-*n*-dialkylazoxybenzenes[22,23] [Fig. 5(a)]. We used $n=5$, 6, 7, and 8 homologues of 4,4′-*n*-dialkylazoxybenzene, purchased from Sigma-Aldrich Chemical Company (St. Louis, MO), to prepare mixtures with a broad temperature range of the SmA phase. All components were purified to decrease the contents of undesired dopants and foreign particles. The purification process was as follows. First, we dissolved the compound in methanol (99.93%, Aldrich) in proportion 1 g of LC in 100 ml of methanol. Then the solution was cooled down to separate the crystal from the methanol. The precipitated crystals were filtered and dried out. The purified compounds were mixed in various proportions to get the appropriate phase sequence and good alignment. The temperature range of SmA phase can be expanded to about 30 deg in eutectic mixtures. The mixture of $n=6$ and $n=8$ homologues in proportion of 1:1 shows the best deflection efficiency (a ratio of intensities of the deflected and incident beams) and a good thermal range [Fig. 5(b)]. These mixtures were used as a SmA filler for passive prismatic deflectors.

3 Optical Elements: Smectic-A-Filled Prisms and Lattices

3.1 *Single Smectic-A prisms*

The geometry of the prismatic cell filled with LC material is shown in Fig. 1. Two glass plates with rubbed polyimide layers (PI2555, Microsystems, Cupertino, CA) formed a wedge cell, which was filled with the SmA blend of 4,4′-dihexylazoxybenzene and 4,4′-dioctylazoxybenzene in proportion of 1:1. The assembled cell was heated to the isotropic state and slowly cooled down to room temperature with the temperature rate $\sim 5\times 10^{-4}$ K/s in 1.2-T magnetic field. The measured parameters of the birefringent prism are as follows:

- wedge angle: 9.2 deg
- refractive indices of the SmA mixture (at $\lambda=633$ nm and temperature 22 °C): $n_e=1.72\pm 0.01$, $n_o=1.53\pm 0.01$, and $\Delta n=0.19$
- steering angles: for the light polarized parallel to the LC director (extraordinary wave) $\theta_e=6.7$ deg; and for the light polarized perpendicular to the LC director (ordinary wave) $\theta_0=4.9$ deg.

The textures of the aligned mixture [Fig. 6(a)] show a

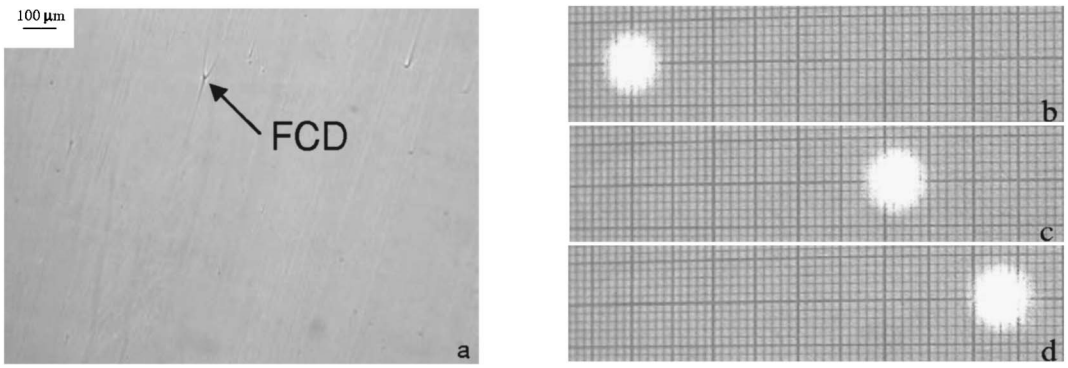

Fig. 6 (a) Texture observations of the wedge cell filled with the SmA mixture after alignment in 1.2-T magnetic field. Thickness of the cell is ~200 μm, wedge angle is ~9.2 deg. (b) Position of the incident beam on the screen. (c) Position of the deflected ordinary beam passed through the wedge cell. (d) Position of the deflected extraordinary beam.

small amount of residual FCDs. As the SmA mixture has a positive birefringence $\Delta n = n_e - n_o > 0$, the extraordinary wave will deflect more than the ordinary wave [Figs. 6(b)–6(d)]. In Fig. 7, we show the transmission of the extraordinary and ordinary waves through the wedge in SmA (t=25 °C) and nematic phases (t=48 °C) at wavelength $\lambda = 633$ nm. The photodetector was placed at a distance 22 cm from the sample. The diameter of the probing laser beam was about 2 mm. The data are normalized by the incident light intensity I_0. Figure 7 clearly demonstrates that the SmA phase is much more transparent than the nematic phase due to reduction of light scattering at the director fluctuations. The transmission of SmA phase remains above 70% for both ordinary and extraordinary components, even when the LC layer becomes thicker than 1 mm. The variations of light transmission with thickness observed in the plots in Fig. 7 for SmA are caused by the residual amount of FCDs in different regions of the wedge-shaped cell used for the measurements.

3.2 *Polymer Array of Prisms Filled with Smectic-A Material*

The assembling of the SmA-filled wedges for the wide-aperture incident beam requires large quantities of LC material. A more practical approach might be to replace a single birefringent prism with an array of smaller prisms, at the expense of some decrease in light transmission efficiency caused by light diffraction, destructive interference, and nonideal profile. Hirabayashi, Yamamoto, and Yamaguchi reported on quartz microprisms filled with the nematic material, which can deflect closely spaced micro-optical beams individually to any position with a high transmit-

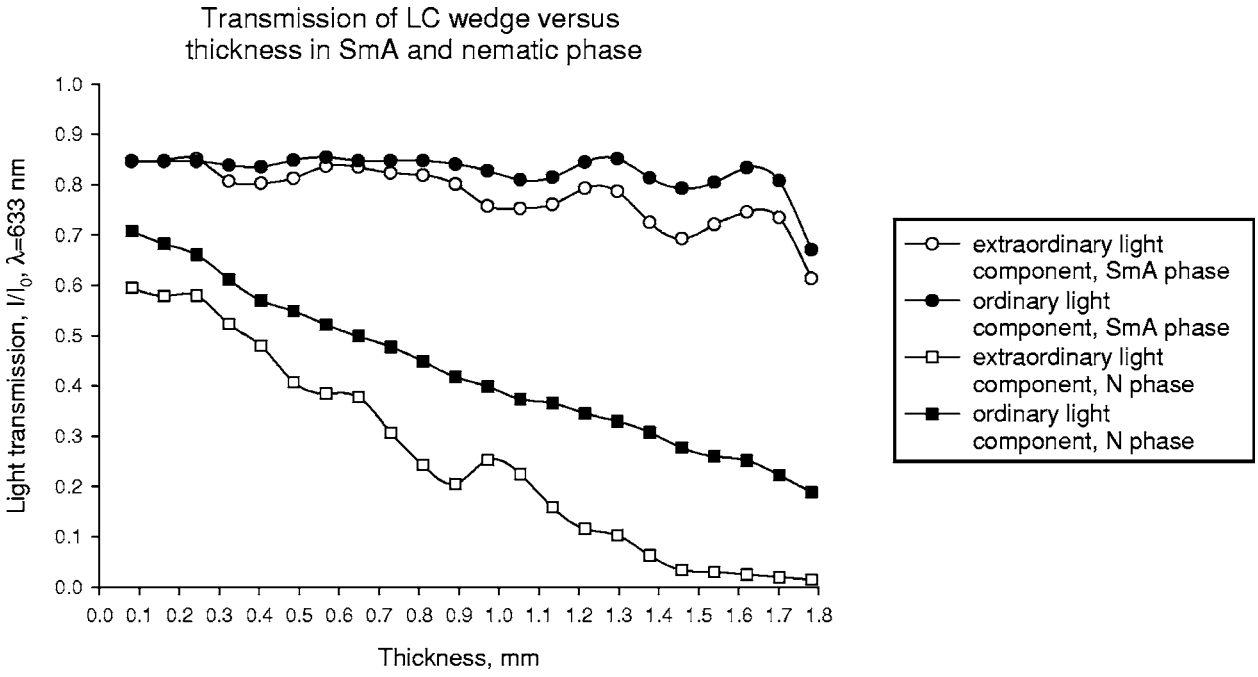

Fig. 7 Transmission of the birefringent wedge cell at $\lambda = 633$ nm.

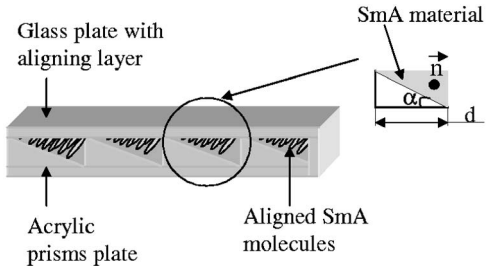

Fig. 8 Sketch of the array of polymer prisms filled with the SmA material.

tance, high deflection angle, and low voltage.[39] Here we describe an array of prisms filled with a SmA material. Right-angle prisms may be molded in a sheet of polymer material with a different cut angle α and period d (Fig. 8). We used an array of prisms formed in an acrylic film of optically quality with the refractive index $n=1.49$ (at $\lambda=589$ nm) with $\alpha=30$ deg and $d=1$ mm (purchased from Fresnel Technologies, Incorporated, Fort Worth, TX). The acrylic array of prisms was attached to a glass substrate coated with rubbed polyimide PI2555 to align the director along the groves. Then the assembled cell was filled with the 1:1 (by weight) mixture of 4,4′-dihexylazoxybenzene and 4,4′-dioctylazoxybenzene. After magnetic field alignment, we measured the deflection efficiency and deflection angles of the cell at 633 nm for normal incidence at room temperature (we considered the zero-order diffracted beam; the diameter of the incident beam was 5 mm; and the cell was illuminated from the glass plate side):

- for the extraordinary wave, the deflection efficiency was ~75.4% and the deflection angle $\theta_e=7.2$ deg±0.2 deg
- for the ordinary wave, the deflection efficiency was ~80.5% and the deflection angle $\theta_o=0.6$ deg±0.2 deg.

The performance of the assembled cell is very similar to Rochon prisms, but due to a slight mismatch between the acrylic refractive index and ordinary refractive index of the LC material, the ordinary wave is slightly deflected. We checked the temperature dependence of the deflection characteristics of SmA-filled microprisms. The temperature-induced changes in the deflection angles were relatively small, about 0.02° per 1 °C for the extraordinary and less than that for the ordinary wave. Thus, with the temperature increase from 15 to 40 °C, the deflection angles changed from 7.14 to 6.68 deg for the extraordinary beam and from 0.61 to 0.56 deg for the ordinary beam.

The light propagation through the array of prisms is affected by the geometry of the prisms, which is far from the ideal triangular profile. In Fig. 9 we show the fluorescent confocal microscopy[40] images of the prisms filled with the mixture of Cargille™ (Cedar Grove, NJ) refractive index fluid ($n_d=1.52$) and Nile Red (Aldrich) fluorescent dye (0.01% by weight). The prisms profile is not regular, which is the reason for the difference (of about 0.2 deg) between the measured and theoretically calculated values of the deflection angles.

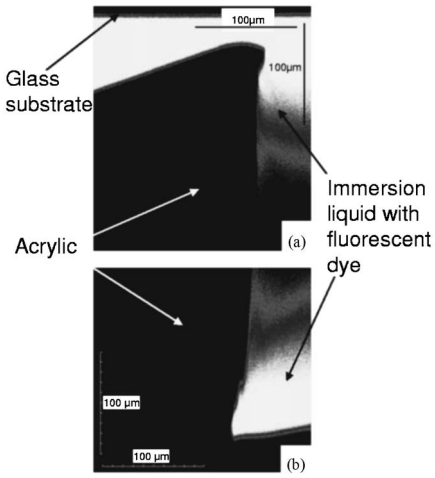

Fig. 9 Confocal microscopy study of the polymer prisms array: (a) apex of one acrylic prism of the array and (b) base of the acrylic prism.

4 Polarization Rotators

We used 90 deg TN cells as electrically controlled polarization rotators. The cells were assembled from two glass plates with indium-tin-oxide (ITO) layers and covered by rubbed polyimide PI2555 (Microsystems), which provides planar orientation of the LC molecules. Easy axes of the nematic director are mutually orthogonal at the opposite substrates. The cells were filled with the mixture of dual-frequency nematic mixture MLC-2048 (Merck, optical birefringence $\Delta n=0.22$ at $\lambda\approx 633$ nm) and right-handed chiral dopant R1011 [Merck (Darmstadt, Germany), 0.05% by weight].

Depending on the applied voltage, the TN cell can be either in the state of OFF or ON (Fig. 1). In the OFF state, the cell rotates the polarization of the linearly polarized beam by 90 deg. The emerging light remains linearly polarized only if the TN cell satisfies one of two criteria: 1. either it is infinitely thick and satisfies the Mauguin limit ($\lambda \ll d\cdot\Delta n$) or 2. its thickness d satisfies the conditions of the so-called Gooch-Tarry or Mauguin minima[41]:

$$d=\frac{\lambda}{2\Delta n}\sqrt{4m^2-1};\quad m=1,2,3,\ldots. \tag{6}$$

In the ON state of the TN cell, the direction of light polarization remains the same. An applied voltage realigns the nematic director perpendicular to the plates and the optical activity disappears. We used the TN cells of thickness $d\approx 5.6$ μm to satisfy the condition of the second minimum[41] at $\lambda=633$ nm. We measured the optical transmission of the TN cells with antireflective coatings at $\lambda=633$ nm. The transmission coefficient (the ratio of the output beam intensity to the incident beam intensity) was 94% for the OFF state and 97% for the ON state.

Figure 10 shows the typical time dependence of the transmission of the TN cell placed between crossed polarizers at $\lambda=633$ nm. The optical signal shows good stability for both ON and OFF states of the TN cell under application of the repetitive driving voltage [Fig. 10(a)]. To avoid a back flow effect (nematic material flows caused by direc-

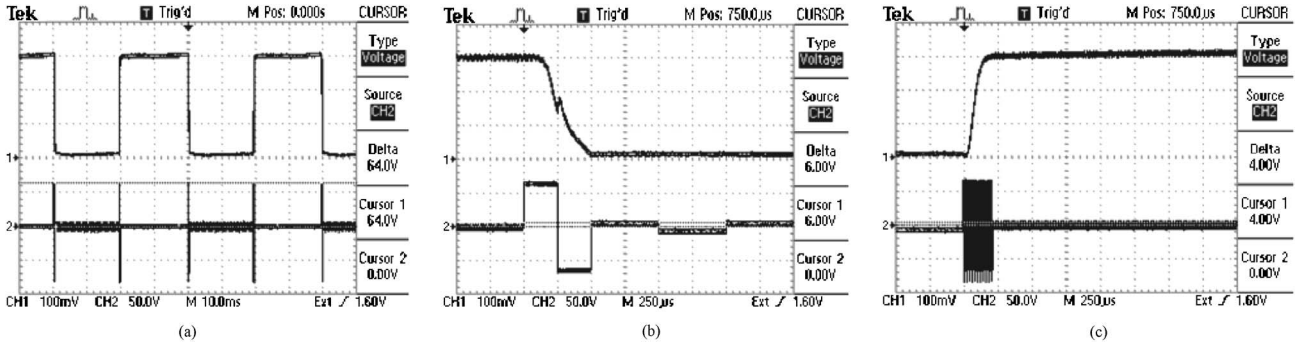

Fig. 10 Oscilloscope pictures demonstrating the optical transmittance of the 90-deg TN cell (top traces) filled with dual-frequency nematic material (crossed polarizers, cell thickness 5.6 μm) versus the applied voltage (bottom traces). (a) Fast linear polarization switching with repetition rate of 25 Hz. Time scale 10 ms/sqr. (b) Transition of TN cell to the homeotropic state by application of the low-frequency kick-off voltage pulses (64-V rms, f=2 kHz), followed by the low-frequency holding voltage (6-V rms, f=1 kHz). Time scale 250 μs/sqr. (c) Transition of TN cell to the planar state by application of the high-frequency kick-off voltage pulses (64-V rms, f=50 kHz), followed by the high-frequency holding voltage (4-V rms, f=50 kHz). Time scale 250 μs/sqr.

tor reorientation), we applied holding and kick-off voltage pulses with properly adjusted amplitudes. For example, we used $U_{\mathrm{rms,hold,1\ kHz}}=6$ V and $U_{\mathrm{rms,hold,50\ kHz}}=4$ V to hold 5.6-μm-thick TN cells in the homeotropic and twisted state, respectively. To minimize a dielectric heating effect, we applied high-amplitude pulses for a short time, 0.5 and 0.25 ms, at frequencies 2 and 50 kHz, respectively. With these pulses, we were driving the TN cell continuously for hours but did not observe a worsening of the transmission signal caused by the dielectric heating effect.

By applying the driving voltage with high-amplitude kick-off voltage pulses, we achieved a switching time of about 0.5 ms for ON [Fig. 10(b)] and about 0.25 ms for OFF [Fig. 10(c)] states. The kick-off voltage pulses are applied either at low (f=2 kHz) or high (f=50 kHz) frequencies, to switch the dual-frequency nematic material into ON or OFF states, respectively (the dielectric anisotropy of MLC-2048 is positive below some critical frequency f_c and negative at $f>f_c$, where $f_c\approx 12$ kHz for MLC-2048 mixture at the temperature 20 °C). The application of an amplitude- and frequency-modulated waveform for driving of a dual-frequency nematic has an obvious advantage in comparison with a conventional nematic driving scheme, where the high-frequency pulses are absent. For example, the response time is only about 30 ms with the same cell when no high-frequency signal is applied and the cell is relaxing from the ON to OFF state due to restoring elastic forces. A much faster switching of 0.25 ms is achieved with application of high-frequency voltage pulses [Fig. 10(c)].

5 Conclusions

We demonstrate the applicability of SmA materials in birefringent prisms and arrays. SmA elements can be used in nonmechanical DBDs that are based on decoupled pairs of electrically controlled liquid crystalline polarization rotators, such as TN cells and passive deflectors. This approach allows one to separate the issue of time response and beam deflection angles and optimize these two parameters separately. We achieve fast (0.5 ms) response time of dual-frequency nematic 90-deg TN cells by implementing an overdriving scheme of electrical switching, where an electrical signal is a sequence of high-amplitude pulses (64-V rms, at 2 and 50 kHz) and holding voltages (6- and 4-V rms at 1 and 50 kHz, respectively).

The deflection angles can be optimized by the design of the birefringent prisms. SmA-filled prisms are attractive in low-cost applications where one needs large apertures, large angles of deflection, and/or nontrivial geometries. We demonstrate that mixtures of homologues of 4,4′-*n*-dialkylazoxybenzene produce SmA phases with a broad temperature range of SmA existence (up to 30 °C for binary mixtures) with a relatively small number of residual defects, such as FCDs and show good transmission characteristics. We determine the typical magnetic fields needed to remove director distortions around the mechanical inclusions and focal conic domains. Magnetic alignment is most effective when the material is aligned in the nematic phase, and then cooled down to the SmA phase.

The SmA-filled birefringent prisms have certain advantages as compared to the crystalline prisms. The SmA prisms are easier and cheaper to form. The optical axis of SmA prisms can be controlled by surface alignment. They can be prepared as relatively thick prisms (up to 7 mm in our case) or as arrays of (micro) prisms. Light scattering in SmA birefringent prisms can be reduced by proper alignment to levels that are significantly lower than light scattering at the director fluctuations in the nematic samples of the same thickness. As the light scattering is caused mostly by FCDs that have a fixed size, it becomes smaller with the increase of the wavelength of light; the IR part of the spectrum is less sensitive to these losses. Thus, the SmA prisms are suitable candidates for beam steering not only in the visible part of the spectrum, but in the infrared part as well. An obvious drawback of the SmA prisms is that they can be used only within the temperature range of the SmA phase. The latter can be expanded significantly by using mixtures, as in this work.

Acknowledgments

We thank Phil Bos and Sergij Shiyanovskii for numerous useful discussions. The work was supported by NASA grant NAG3-2539 and by Rockwell Scientific Company.

References

1. P. F. McManamon, E. A. Watson, T. A. Dorschner, and L. J. Barnes, "Applications look at the use of liquid-crystal writable gratings for steering passive radiation," *Opt. Eng.* **32**(11), 2657–2664 (1993).
2. J. A. Thomas and Y. Fainman, "Optimal cascade operation of optical phased-array beam deflectors," *Appl. Opt.* **37**(26), 6196–6212 (1998).
3. O. Solgaard, F. S. A. Sandejas, and D. M. Bloom, "Deformable grating optical modulator," *Opt. Lett.* **17**(9), 688–690 (1992).
4. R. Fuchs, H. Jerominek, N. Swart, Y. Diawara, M. Lehoux, G. Bilodeau, S. Savard, F. Cayer, Y. Rouleau, and P. Lemire, "Novel beam steering micromirror device," *Proc. SPIE* **3513**, 40–49 (1998).
5. J. H. Kim, L. Sun, C. H. Jang, C. C. Choi, and R. T. Chen, "Polymer-based thermo-optic waveguide beam deflector with novel dual folded-thin-strip heating electrodes," *Opt. Eng.* **42**(3), 620–624 (2003).
6. D. Kang, J. E. Maclennan, N. A. Clark, A. Zakhidov, and R. H. Baughman, "Electro-optic behavior of liquid-crystal-filled silica opal photonic crystals: Effect of liquid-crystal alignment," *Phys. Rev. Lett.* **86**(18), 4052–4055 (2001).
7. W. Klaus, "Development of LC optics for free-space laser communications," *AEU, Int. J. Electron. Commun.* **56**(4), 243–253 (2002).
8. S. T. Wu, M. E. Neubert, S. S. Keast, D. G. Abdallah, S. N. Lee, M. E. Walsh, and T. A. Dorschner, "Wide nematic range alkenyl diphenyldiacetylene liquid crystals," *Appl. Phys. Lett.* **77**(7), 957–959 (2000).
9. A. B. Golovin, S. V. Shiyanovskii, and O. D. Lavrentovich, "Fast-switching dual-frequency liquid crystal optical retarder, driven by an amplitude and frequency modulated voltage," *Appl. Phys. Lett.* **83**(19), 3864–3866 (2003).
10. J. Borel, J. C. Deutsch, G. Labrunie, and J. Robert, "Liquid crystal diffraction grating," U.S. Patent No. 3,843,231 (Oct. 1974).
11. G. Williams, N. J. Powell, A. Purvis, and M. G. Clark, "Electrically controlled liquid crystal Fresnel lens," *Proc. SPIE* **1168**, 352–357 (1989).
12. B. J. Cassarly, J. C. Ehlert, and D. J. Henry, "Low insertion loss high precision liquid crystal optical phased array," *Proc. SPIE* **1417**, 110–121 (1991).
13. X. Wang, D. Wilson, R. Muller, P. Maker, and D. Psaltis, "Liquid-crystal blazed-grating beam deflector," *Appl. Opt.* **39**(35), 6545–6555 (2000).
14. C. M. Titus, J. R. Kelly, E. C. Gartland, S. V. Shiyanovskii, J. A. Anderson, and P. J. Bos, "Asymmetric transmissive behavior of liquid-crystal diffraction gratings," *Opt. Lett.* **26**(15), 1188–1190 (2001).
15. R. L. Sutherland, V. P. Tondiglia, L. V. Natarajan, T. J. Bunning, and W. W. Adams, "Electrically switchable volume holographic gratings in polymer-dispersed liquid crystals," *Appl. Phys. Lett.* **64**(9), 1074–1076 (1994).
16. P. Berthele, E. Gros, B. Fracasso, and J. L. D. De la Tochnaye, "Efficient beam steering in the 1.55 micron window using large-tilt FLC one dimensional array," *Ferroelectrics* **214**(1,2), 791–798 (1998).
17. D. Subacius, S. V. Shiyanovskii, P. Bos, and O. D. Lavrentovich, "Cholesteric gratings with field-controlled period," *Appl. Phys. Lett.* **71**(23), 3323–3325 (1997).
18. A. Y. G. Fuh, C. H. Lin, and C. Y. Huang, "Dynamic pattern formation and beam steering characteristics of cholesteric gratings," *Jpn. J. Appl. Phys., Part 1* **41**(1), 211–218 (2002).
19. U. J. Schmidt, "A high speed digital light beam deflector," *Phys. Lett.* **12**(3), 205–206 (1964).
20. W. Kulchke, K. Kosanke, E. Max, M. A. Haberger, T. J. Harris, and H. Fleisher, "Digital light deflectors," *Appl. Opt.* **5**(10), 1657–1667 (1966).
21. H. Meyer, D. Riekmann, K. P. Schmidt, U. J. Schmidt, M. Rahlff, E. Schroder, and W. Thust, "Design and performance of a 20-stage digital light beam deflector," *Appl. Opt.* **11**(8), 1732–1736 (1972).
22. C. M. Titus, P. J. Bos, O. D. Lavrentovich, "Efficient accurate liquid crystal digital light deflector," *Proc. SPIE* **3633**, 244–253 (1999).
23. C. M. Titus, "Refractive and diffractive liquid crystal beam steering devices," Dissertation, Chemical Physics Interdisciplinary Program, Kent State Univ., pp. 34–36 (2000).
24. D. F. Gu, B. Winker, D. Taber, J. Cheung, Y. Lu, P. Kobrin, and Z. Zhuang, "Dual frequency liquid crystal devices for infrared electro-optical applications," *Proc. SPIE* **4799**, 37 (2002).
25. S. A. Khan and N. A. Riza, "Demonstration of 3-dimensional wide angle laser beam scanner using liquid crystals," *Opt. Express* **12**(5), 868–882 (2004).
26. O. Pishnyak, L. Kreminska, O. D. Lavrentovich, J. J. Pouch, F. A. Miranda, and B. K. Winker, "Digital beam steering device based on decoupled birefringent prism deflector and polarization rotator," NASA/TM-2004-213197.
27. L. M. Blinov and V. G. Chigrinov, *Electrooptic Effects in Liquid Crystal Materials*, Springer-Verlag, New York (1994).
28. P. G. de Gennes and J. Prost, *The Physics of Liquid Crystals*, 2nd ed., Clarendon Press, Oxford (1993).
29. G. Vertogen and W. H. de Jeu, *Thermotropic Liquid Crystals, Fundamentals*, Springer-Verlag, Berlin (1988).
30. M. Kleman and O. D. Lavrentovich, *Soft Matter Physics: An Introduction*, Springer, New York, NY (2003).
31. G. R. Luckhurst, "Field-induced alignment of the directors in the smectic A phase. Experiment and simulation," *Mol. Cryst. Liq. Cryst. Sci. Technol., Sect. A* **347**(2), 121–135 (2000).
32. G. R. Luckhurst, T. Miyamoto, A. Sugimura, and B. A. Timimi, "Electric field-induced alignment of the directors in the smectic A phase of 4-Octyl-4′-Cyanobiphenyl. A deuterium NMR study," *Mol. Cryst. Liq. Cryst. Sci. Technol., Sect. A* **347**(2), 147–156 (2000).
33. Y. Takanishi, Y. Ouichi, H. Takezoe, and A. Fukuda, "Chevron layer structure in smectic A phase of 8CB," *Jpn. J. Appl. Phys., Part 2* **28**(3), L487–489 (1989).
34. O. Ou Ramdane, P. Auroy, S. Forget, E. Raspaud, P. Martinot-Lagarde, and I. Dozov, "Memory-free conic anchoring of liquid crystals on a solid substrate," *Phys. Rev. Lett.* **84**(17), 3871–3874 (1994).
35. O. D. Lavrentovich, M. Kleman, and V. M. Pergamenshchik, "Nucleation of focal conic domains in smectic A liquid crystals," *J. Phys. II* **4**(2), 377–404 (1994).
36. O. D. Lavrentovich and M. Kleman, "Field-driven first-order structural transition in the restricted geometry of a smectic A cell," *Phys. Rev. E* **48**(1), R39-R42 (1993).
37. M. Kleman and O. D. Lavrentovich, "Curvature energy of a focal conic domain with arbitrary eccentricity," *Phys. Rev. E* **61**(2), 1574–1578 (2000).
38. Z. Li and O. D. Lavrentovich, "Surface anchoring and growth pattern of the field-driven first-order transition in a smectic-A liquid crystal," *Phys. Rev. Lett.* **73**(2), 280–283 (1994).
39. K. Hirabayashi, T. Yamamoto, and M. Yamaguchi, "Free-space optical interconnections with liquid-crystal microprism arrays," *Appl. Opt.* **34**(14), 2571–2580 (1995).
40. I. I. Smalyukh, S. V. Shiyanovskii, and O. D. Lavrentovich, "Three-dimensional imaging of orientational order by fluorescence confocal polarizing microscopy," *Chem. Phys. Lett.* **336**, 88–96 (2001).
41. C. H. Gooch and H. A. Tarry, "The optical properties of twisted nematic liquid crystal structures with twist angles ⩽90°," *J. Phys. D* **8**(13), 1575–1584 (1975); and C. H. Gooch and H. A. Tarry, "Optical characteristics of twisted nematic liquid-crystal films," *Electron. Lett.* **10**(1), 2–4 (1974).

Oleg Pishnyak received his MS degree in physics with a major in optics in 1997 from Chernivtsi National University, Ukraine. His research interests include phase separation in liquid crystal/polymer systems, electro-optic applications of liquid crystals, and the design and characterization of beam-steering devices. Currently he is a graduate student at the Liquid Crystal Institute, Department of Chemical Physics of Kent State University, Ohio.

Andrii Golovin received his MS degree in optical and electrical engineering from the physics department of Kiev State University, Ukraine, in 1987. He received his PhD in optics and laser physics from the Institute of Physics, Ukrainian Academy of Sciences, Kiev, Ukraine, in 1994. He currently works at the Liquid Crystal Institute at Kent State University, Ohio. His research interests include optics, lasers, and liquid crystals.

Liubov Kreminska received her PhD in optics and laser physics in 1997 from the Institute of Physics, the National Academy of Sciences of Ukraine, Kiev, and MS in physics in 1987 from Kiev State University, Ukraine. She accomplished postdoctoral research at the Liquid Crystal Institute, Kent State University, Ohio. Her areas of research interest are optics of singularities and applied optics of liquid crystals. She is currently an assistant professor of physics at Truman State University.

John J. Pouch received a BSc degree in physics (1975) and a PhD in solid state physics (1981) from Wayne State University. Since 1983, he has been employed at the NASA Glenn Research Center (GRC), Cleveland, Ohio. He has conducted research in the areas of plasmas and surface science. His discovery of a reactive ion etching process enabled GRC's silicon carbide thin film group to fabricate NASA's first operational diode based on this material. He has co-authored more than 50 technical publications, and more than 80 conference presentations. He is the co-editor of five scientific books and two conference proceedings. He currently oversees emerging programs based on radio-frequency communications technologies.

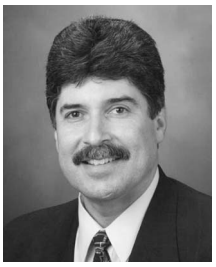

Félix A. Miranda received his BS degree in physics from the University of Puerto Rico in 1983, an MS degree in physics from Rensselaer Polytechnic Institute in 1986, and a PhD degree in physics from Case Western Reserve University in 1991. He is currently the chief of the antenna, microwave, and optical systems branch in the communications technology division. His areas of expertise are antenna technology, ferroelectric tunable microwave components, microwave integrated circuits, and devices for space and ground-based communications. He is a senior member of the Institute of Electrical and Electronics Engineers (IEEE), a member of the American Physical Society (APS), a member of the Society of Hispanic Professional Engineers (SHPE), a member of the Materials Research Society (MRS), and a member of the Forum of Industrial and Applied Physicists (FIAP). He is on the editorial board of *Integrated Ferroelectrics* (Taylor and Francis). He has authored or co-authored more than 130 technical publications in his areas of expertise. He has written several book chapters and is the co-inventor of four U.S. patents, with one additional patent pending. He is a former NASA Administrator's Fellow, received the 2001 Outstanding Technical Achievement Award from the Hispanic Engineer National Achievement Awards Conference (HENAAC), and the 2005 NASA Space Act Award for the development of an Antenna Near-Field Probe Station Scanner.

Bruce K. Winker: biography and photograph not available.

Oleg D. Lavrentovich received his PhD (1984) and Doctor of Sciences (1981) degrees, both in physics and mathematics, from the Academy of Sciences, Institute of Physics, Kiev, Ukraine. He has conducted research in the area of liquid crystals, their structural, electro-optical, and surface properties. He has authored and co-authored more than 130 research publications and wrote (with M. Kleman) a textbook *Soft Matter Physics: An Introduction* (Springer, New York, 2003). He is a member of the editorial board of *Physical Review E* and a Fellow of SPIE. He is director of the Liquid Crystal Institute and Chemical Physics Interdisciplinary Program at Kent State University, Ohio.